

## Monte Carlo renormalization group study of crosslinked polymer chains on fractals

This article has been downloaded from IOPscience. Please scroll down to see the full text article.

1998 J. Phys. A: Math. Gen. 31 1365

(<http://iopscience.iop.org/0305-4470/31/5/007>)

View [the table of contents for this issue](#), or go to the [journal homepage](#) for more

Download details:

IP Address: 171.66.16.104

The article was downloaded on 02/06/2010 at 07:21

Please note that [terms and conditions apply](#).

# Monte Carlo renormalization group study of crosslinked polymer chains on fractals

Ivan Živić† and Sava Milošević‡

† Faculty of Natural Sciences and Mathematics, University of Kragujevac, 34000 Kragujevac, Serbia, Yugoslavia

‡ Faculty of Physics, University of Belgrade, PO Box 368, 11001 Belgrade, Serbia, Yugoslavia

Received 1 July 1997, in final form 30 September 1997

**Abstract.** We study the problem of two crosslinked polymer chains in a good solvent, modelled by two mutually crossing self-avoiding walks situated on fractals that belong to the Sierpinski gasket (SG) family (whose members are labelled by an integer  $b$ ,  $2 \leq b \leq \infty$ ). By applying the Monte Carlo renormalization group (MCRG) method, we calculate the critical exponent  $\gamma$  associated with the number of crossings of the two self-avoiding-walk paths, for a sequence of SG fractals with  $2 \leq b \leq 100$ . For the problem under study, we find that our MCRG approach provides results that are virtually rigorous, that is, results with exceptionally small deviations (at most 0.07%) from the available ( $2 \leq b \leq 5$ ) exact renormalization group results. We discuss our set of MCRG data for  $\gamma$  as a function of the fractal parameter  $b$ , and compare its behaviour with the finite-size scaling predictions.

## 1. Introduction

The self-avoiding walk (SAW) is a random walk that must not contain self-intersections. It has been extensively used as a model of a linear polymer chain in a good solvent. Although an isolated chain is difficult to observe experimentally (even at high polymer dilution), numerous studies of single-chain statistics have been upheld as an essential step towards understanding more challenging many-chain systems. A simple-minded extension of the single polymer concept is the model of two chains in a solvent (good for both chains) [1] whose properties can be also investigated by studying statistics of two SAWs on a lattice. However, the corresponding investigations are difficult because of the presence of interchain interactions. In this paper we study the case of two chemically different polymers that have a pronounced crosslinking interaction. Such a situation can be modelled by two mutually crossing self-avoiding walks (MCSAW), that is, by two SAWs whose paths on a lattice can cross (intersect) each other, which, in the case of two-dimensional SAWs, can be associated with two entangled wigglers (on a tabletop) that can cross over each other. With each crossing we may associate the contact energy  $\epsilon_c$ , and, in analogy with the problem of polymer interaction with a penetrable surface [2], we may assume that with decreasing temperature the number of crossings  $M$  increases so that at the critical temperature  $T_c$  it behaves according to the power law

$$M \sim N^\gamma \quad (1)$$

where  $N$  is the total number of monomers in the longer chain. Below  $T_c$  the number of crossings becomes proportional to  $N$ , whereas above  $T_c$  it is vanishingly small.

The problem of two chemically different polymers in a good solvent has been extensively studied experimentally [3–5] and theoretically. Various theoretical techniques have been applied, including the random phase approximation [1, 6–8], renormalization group (RG) methods [9–12], field theoretical approach [13] and Monte Carlo simulations [14], to study models of the polymer system on Euclidean lattices. However, in spite of these numerous different studies of the polymer problem in the case of the Euclidean lattices, the entire physical picture achieved so far is of a phenomenological character and, for example, there is no exact result for the contact critical exponent  $\gamma$ . For this reason, it is desirable to extend the relevant study to a family of fractal lattices whose members allow, in principle, exact treatment of the problem and whose characteristics approach (via the so-called fractal-to-Euclidean crossover) properties of a Euclidean lattice. Moreover, the study of the polymer problem on fractal lattices has its own practical importance because real containers of the polymer solvent are in many cases porous media that are often fractals, which means that they display self-similar distribution of voids (obstacles) over three to four orders of magnitudes in length scale.

The case of a single polymer chain or, more precisely, asymptotic properties of SAWs, on the first member (labelled by  $b = 2$ ) of the infinite Sierpinski gasket (SG) fractal family was studied by means of an exact RG approach in the pioneering work of Dhar [15]. This exact study was later extended [16] to the case of a finite sequence ( $3 \leq b \leq 8$ ) of the SG family. In an analogous way, Kumar and Singh [17, 18] have recently studied the polymer problem described by the MCSAW model situated on the SG family of fractals. They have applied an exact RG approach, in the case of the first four ( $2 \leq b \leq 5$ ) members of the infinite SG family of fractals, to calculate the contact exponent  $\gamma$ , while for the fractal-to-Euclidean crossover region, that is, for large  $b$  members of the SG fractal family, they have propounded a finite-size scaling approach formula for  $\gamma$ .

In this paper we exploit the Monte Carlo renormalization group (MCRG) method to calculate the contact critical exponent  $\gamma$  for the MCSAW model situated on the SG fractals. We have obtained  $\gamma$  for a long sequence of the SG fractals, that is, for  $2 \leq b \leq 100$ . Comparing our results for  $2 \leq b \leq 5$  with the exact RG results [17, 18], we find that there is no deviation larger than 0.07% and, for this reason, we can accept the entire set of MCRG results as very reliable. Details of the performed MCRG calculations are explained in section 2. In section 3 we present an overall discussion of our findings within the framework of the current knowledge of the properties of two interpenetrating polymers.

## 2. The MCRG approach

In this section we are going to apply the MCRG method to the MCSAW model on the SG family of fractals. These fractals have been studied in numerous papers so far, and consequently we shall give here only a requisite brief account of their basic properties. It starts with recalling the fact that each member of the SG fractal family is labelled by an integer  $b \geq 2$  and can be constructed in stages. At the first stage ( $r = 1$ ) of the construction there is an equilateral triangle (generator) that contains  $b^2$  identical smaller triangles of unit side length, out of which only the upper oriented are physically present. The subsequent fractal stages are constructed recursively, so that the complete self-similar fractal lattice is obtained in the limit  $r \rightarrow \infty$ . Therefore, the fractal dimension of the complete SG fractal appears to be  $d_f = \ln[b(b + 1)/2] / \ln b$ .

In the terminology that applies to the SAW, we assign the weight  $x_1$  to a step of one SAW and the weight  $x_2$  to a step of the other walk. In order to explore effects of crosslinking of two SAWs on the SG fractals, we introduce the two Boltzmann factors  $w = e^{-\epsilon_c/T}$  and

$t = e^{-\epsilon_c/T}$ , where  $\epsilon_c$  is energy of two monomers in contact (which occurs at a crossing site of SAWs), while  $\epsilon_t$  is the energy associated with two sites which are nearest neighbours to a crosslinked site and which are visited by different SAWs (see figure 1). Here we set the Boltzmann constant  $k_B$  equal to unity.

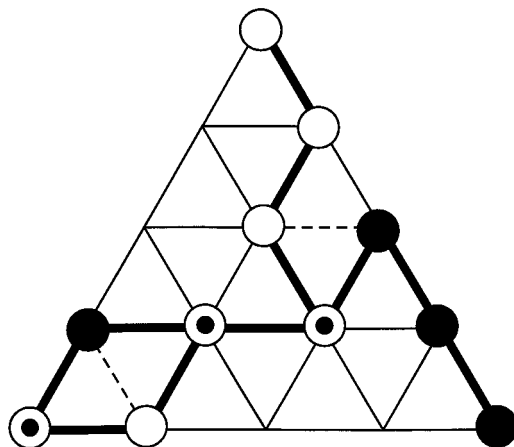


**Figure 1.** The  $b = 4$  fractal generator with segments of two different SAW chains (two different polymers) depicted by open and full circles. The two SAWs cross each other at the three sites (marked by small full circles within bigger open circles), with which we associate the interaction energy  $\epsilon_c$ . The dotted bonds indicate interaction, with energy  $\epsilon_t$ , between different sites (monomers) which are nearest neighbours to crosslinked points. Thus, for example, the presented two-SAW configuration should contribute the weight  $x_1^6 x_2^6 w^3 t^2$  in the corresponding RG equations (more specifically, in equation (5) for  $r = 0$ ).

Important aspects of the statistics of the two-chain polymer system, described by the MCSAW model, can be learnt by introducing four restricted partition functions  $B_1^{(r)}$ ,  $B_2^{(r)}$ ,  $C^{(r)}$ , and  $D^{(r)}$ , that are depicted in figure 2. The recursive nature of the fractal construction imply the following recursion relations for the restricted partition functions

$$B_1^{(r+1)} = \sum_{N_{B_1}} B_{N_{B_1}} (B_1^{(r)})^{N_{B_1}} \tag{2}$$

$$B_2^{(r+1)} = \sum_{N_{B_2}} B_{N_{B_2}} (B_2^{(r)})^{N_{B_2}} \tag{3}$$

$$C^{(r+1)} = \sum_{N_{B_1}, N_{B_2}, N_C, N_D} C_{N_{B_1}, N_{B_2}, N_C, N_D} (B_1^{(r)})^{N_{B_1}} (B_2^{(r)})^{N_{B_2}} (C^{(r)})^{N_C} (D^{(r)})^{N_D} \tag{4}$$

$$D^{(r+1)} = \sum_{N_{B_1}, N_{B_2}, N_C, N_D} D_{N_{B_1}, N_{B_2}, N_C, N_D} (B_1^{(r)})^{N_{B_1}} (B_2^{(r)})^{N_{B_2}} (C^{(r)})^{N_C} (D^{(r)})^{N_D} \tag{5}$$

where the coefficients  $B_{N_{B_1}}$  (and equally  $B_{N_{B_2}}$ ),  $C_{N_{B_1}, N_{B_2}, N_C, N_D}$ , and  $D_{N_{B_1}, N_{B_2}, N_C, N_D}$  are not functions of  $r$ , and each of them represents the number of ways in which the corresponding parts of the two-SAW configuration, within the  $(r + 1)$ th stage fractal structure, can be comprised of the two-SAW configurations within the fractal structures of the next lower order. Because of the independence of  $r$ , these coefficients can be calculated by studying all mutually crossing SAW paths within the fractal generator only.

The above set of relations (2)–(5), can be considered as the RG equations for the problem under study, with the corresponding initial conditions:  $B_1^{(0)} = x_1$ ,  $B_2^{(0)} = x_2$ ,

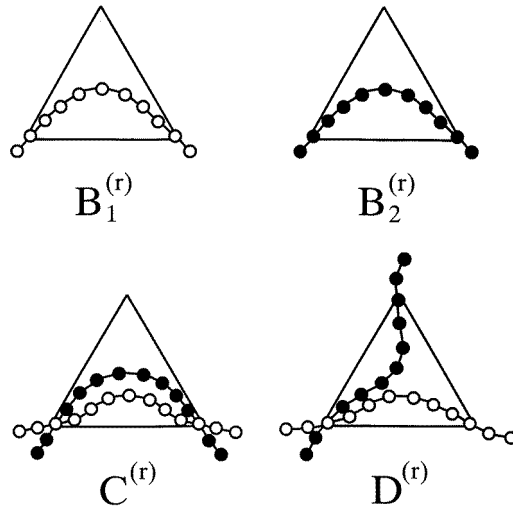


**Figure 2.** A schematic representation of the four basic restricted partition functions (for an  $r$ th stage fractal structure) used to construct all possible configurations of two chain polymers described by the MCSAW model. Monomers of one polymer are depicted by open circles, while monomers of the other polymer are depicted by full circles.

$C^{(0)} = x_1 x_2 w^2$ , and  $D^{(0)} = x_1 x_2 w t$ . On physical grounds, one can expect that these RG equations should have three relevant fixed points ( $B_1^*$ ,  $B_2^*$ ,  $C^*$ ,  $D^*$ ) of the type  $(B^*, B^*, 0, 0)$ ,  $(B^*, B^*, (B^*)^2, (B^*)^2)$ , and  $(0, 0, B^*, 0)$  [17]. The first fixed point with  $C^* = 0$  and  $D^* = 0$ , due to the meaning of these quantities (see figure 2), describes the segregated phase of two chain polymers that should be expected in the high-temperature region. Conversely, the third fixed point, with  $B_1^* = B_2^* = 0$  and  $D^* = 0$ , describes the polymer entangled state, which should appear at low temperatures. Finally, the second fixed point (with  $B_1^* = B_2^* = B^*$  and  $C^* = D^* = (B^*)^2$ ) describes the state of the two-polymer system that occurs at the critical temperature  $T = T_c$  when segregated and entangled polymer phases become identical. This fixed point appears to be a tricritical point, which may be verified by studying numerically the behaviour of the pertinent derivatives of the singular part of the free energy, in the same way as has been carried out in the case of the single polymer adsorption problem on fractal lattices [19–21]. In what follows we focus our attention on the tricritical fixed point in order to calculate the contact critical exponent  $\gamma$ . It should be observed that equations (2) and (3), for each  $b$ , have only one non-trivial fixed point value  $B^*$  [19], which thereby completely determines the tricritical fixed point.

Calculation of the contact critical exponent  $\gamma$  starts with solving the eigenvalue problem of the RG equations (2)–(5) linearized at the tricritical fixed point. Hereafter, we are going to use the prime symbol as a superscript for the  $(r + 1)$ th restricted partition functions and no indices for the  $r$ th-order partition functions. In proceeding further it should be noticed that the RG equations (2) and (3) have identical structure and, in addition, they are not coupled with the other two RG equations, which implies that the eigenvalue problem can be separated into two parts. The first part of the eigenvalue problem, related to equation (2) (or (3)) gives the eigenvalue of the end-to-end distance critical exponent ( $\nu = \ln b / \ln \lambda_\nu$ )

$$\lambda_\nu = \left. \frac{\partial B_1'}{\partial B_1} \right|_* = \left. \frac{\partial B_2'}{\partial B_2} \right|_* \quad (6)$$

where the asterisk denotes that the derivatives should be taken at the tricritical fixed point. The second part of the eigenvalue problem reduces to solving the equation

$$\left| \begin{pmatrix} \left(\frac{\partial C'}{\partial C} - \lambda\right) & \frac{\partial C'}{\partial D} \\ \frac{\partial D'}{\partial C} & \left(\frac{\partial D'}{\partial D} - \lambda\right) \end{pmatrix} \right|^* = 0 \tag{7}$$

which, in general, gives two additional eigenvalues for each  $b$ , but in practice it turns out that only one of them (to be denoted by  $\lambda_y$  from now on) is relevant ( $\lambda_y > 1$ ). Knowing  $\lambda_y$ , we can determine the critical exponent  $y$  [17] through the formula

$$y = \frac{\ln \lambda_y}{\ln \lambda_v} \tag{8}$$

Hence, in an exact RG evaluation of  $y$  one needs to calculate partial derivatives of sums (2)–(5), and thereby one should find the coefficients  $B_{N_{B_1}}$ ,  $B_{N_{B_2}}$ ,  $C_{N_{B_1}, N_{B_2}, N_C, N_D}$ , and  $D_{N_{B_1}, N_{B_2}, N_C, N_D}$  by an exact enumeration of all possible SAWs for each particular  $b$ , which has been accomplished [17, 18] for the SG fractals with  $b \leq 5$ . However, for large  $b$  the exact enumeration turns out to be a forbidding task. We have circumvented this problem by applying the MCRG method. Within this method, the first step would be to locate the tricritical fixed point. To this end, we may observe that the results obtained in [22, 23] provide information for both  $B^*$  and  $\lambda_v$  for a sequence with  $2 \leq b \leq 100$ . Accordingly, the next step in the MCRG method consists of finding  $\lambda_y$  without explicit calculation of the RG equation coefficients.

To solve the partial eigenvalue problem (7), so as to learn  $\lambda_y$ , we need to find the requisite partial derivatives. These derivatives can be related to various averages of the numbers  $N_C$  and  $N_D$  of different crossings of the SAWs for various two-SAW (two-polymer) configurations that correspond to the restricted partition functions  $C^{(r)}$  and  $D^{(r)}$  (see figure 2). For instance, starting with (4) (in the notation that does not use the superscripts  $(r + 1)$  and  $r$ ) and by differentiating it with respect to  $C$  we get

$$\frac{\partial C'}{\partial C} = \sum_{N_{B_1}, N_{B_2}, N_C, N_D} N_C C_{N_{B_1}, N_{B_2}, N_C, N_D} (B_1)^{N_{B_1}} (B_2)^{N_{B_2}} (C)^{N_C-1} (D)^{N_D} \tag{9}$$

Now, it is convenient to think of  $C'$  as the grand canonical partition function for the ensemble of all possible two SAWs that start at the lower left vertex of the generator and exit at the lower right vertex. With this concept in mind, we can write the corresponding ensemble average

$$\begin{aligned} \langle N_C(B_1, B_2, C, D) \rangle_{C'} &= \frac{1}{C'} \sum_{N_{B_1}, N_{B_2}, N_C, N_D} N_C C_{N_{B_1}, N_{B_2}, N_C, N_D} \\ &\times (B_1)^{N_{B_1}} (B_2)^{N_{B_2}} (C)^{N_C} (D)^{N_D} \end{aligned} \tag{10}$$

which can be directly measured in a Monte Carlo simulation. Combining (9) and (10) we can express the requisite partial derivative in terms of the measurable quantity

$$\frac{\partial C'}{\partial C} = \frac{C'}{C} \langle N_C(B_1, B_2, C, D) \rangle_{C'} \tag{11}$$

In a similar way, we can get the additional three derivatives

$$\frac{\partial C'}{\partial D} = \frac{C'}{D} \langle N_D(B_1, B_2, C, D) \rangle_{C'} \tag{12}$$

$$\frac{\partial D'}{\partial C} = \frac{D'}{C} \langle N_C(B_1, B_2, C, D) \rangle_{D'} \tag{13}$$

$$\frac{\partial D'}{\partial D} = \frac{D'}{D} \langle N_D(B_1, B_2, C, D) \rangle_{D'}. \quad (14)$$

Consequently, calculating the above derivatives at the tricritical fixed point and solving the eigenvalue equation (7) we obtain

$$\lambda_y = \frac{\langle N_C \rangle_{C'}^* + \langle N_D \rangle_{D'}^*}{2} + \sqrt{\left( \frac{\langle N_C \rangle_{C'}^* - \langle N_D \rangle_{D'}^*}{2} \right)^2 + \langle N_C \rangle_{D'}^* \langle N_D \rangle_{C'}^*} \quad (15)$$

which means that  $\lambda_y$  has been expressed in terms of quantities that are all measurable through Monte Carlo simulations. Indeed, the quantities  $\langle N_C \rangle_{C'}^*$ ,  $\langle N_D \rangle_{D'}^*$ ,  $\langle N_C \rangle_{D'}^*$ , and  $\langle N_D \rangle_{C'}^*$  can be directly measured via Monte Carlo simulations. Similarly, it can be argued [22] that the eigenvalue  $\lambda_y$  is equal to  $\langle N_{B_1} \rangle_{B_1}^*$  (or  $\lambda_y = \langle N_{B_2} \rangle_{B_2}^*$ ). The pertinent Monte Carlo techniques have been detailed in [22, 23], and we will not elaborate on them in this paper.

### 3. Results and discussion

The MCRG results for the evaluated averages  $\langle N_{B_1} \rangle_{B_1}^*$ ,  $\langle N_{B_2} \rangle_{B_2}^*$ ,  $\langle N_C \rangle_{C'}^*$ ,  $\langle N_D \rangle_{D'}^*$ ,  $\langle N_C \rangle_{D'}^*$ ,  $\langle N_D \rangle_{C'}^*$ , and for the contact critical exponent  $y$  are given in table 1. The first four results ( $2 \leq b \leq 5$ ) for  $y$  should be compared with the corresponding exact RG results  $y_{b=2} = 0.7491$ ,  $y_{b=3} = 0.7246$ ,  $y_{b=4} = 0.7117$ , and  $y_{b=5} = 0.7042$  obtained in [17,18].

**Table 1.** The MCRG results for the measured averages  $\langle N_{B_1} \rangle_{B_1}^*$ ,  $\langle N_{B_2} \rangle_{B_2}^*$ ,  $\langle N_C \rangle_{C'}^*$ ,  $\langle N_D \rangle_{D'}^*$ ,  $\langle N_C \rangle_{D'}^*$ ,  $\langle N_D \rangle_{C'}^*$ , and for the contact critical exponent  $y$ . Each entry of the table has been obtained by performing one million of the requisite Monte Carlo simulations.

$b$	$\langle N_{B_1} \rangle_{B_1}^* = \langle N_{B_2} \rangle_{B_2}^*$	$\langle N_C \rangle_{C'}^*$	$\langle N_D \rangle_{D'}^*$	$\langle N_C \rangle_{D'}^*$	$\langle N_D \rangle_{C'}^*$	$y$
2	2.3822 ± 0.0006	1.200 ± 0.003	0.946 ± 0.003	0.472 ± 0.001	1.293 ± 0.001	0.7493 ± 0.0067
3	3.991 ± 0.001	1.500 ± 0.003	1.647 ± 0.002	0.808 ± 0.002	1.641 ± 0.002	0.7247 ± 0.0031
4	5.807 ± 0.002	1.814 ± 0.004	1.280 ± 0.002	1.096 ± 0.002	2.019 ± 0.003	0.7123 ± 0.0024
5	7.793 ± 0.003	2.126 ± 0.003	2.889 ± 0.003	1.348 ± 0.003	2.408 ± 0.003	0.7041 ± 0.0017
6	9.937 ± 0.004	2.428 ± 0.004	3.479 ± 0.004	1.598 ± 0.003	2.817 ± 0.004	0.6999 ± 0.0016
7	12.232 ± 0.005	2.727 ± 0.005	4.055 ± 0.004	1.842 ± 0.004	3.220 ± 0.004	0.6962 ± 0.0015
8	14.673 ± 0.007	3.023 ± 0.005	4.645 ± 0.005	2.064 ± 0.004	3.641 ± 0.005	0.6936 ± 0.0013
9	17.232 ± 0.009	3.322 ± 0.005	5.192 ± 0.005	2.298 ± 0.004	4.036 ± 0.006	0.6911 ± 0.0012
10	19.905 ± 0.008	3.609 ± 0.006	5.757 ± 0.006	2.527 ± 0.005	4.475 ± 0.006	0.6902 ± 0.0011
11	22.74 ± 0.01	3.882 ± 0.006	6.320 ± 0.007	2.749 ± 0.005	4.915 ± 0.007	0.6887 ± 0.0011
12	25.64 ± 0.01	4.161 ± 0.007	6.917 ± 0.008	2.982 ± 0.006	5.360 ± 0.009	0.6888 ± 0.0011
13	28.67 ± 0.02	4.471 ± 0.008	7.430 ± 0.008	3.216 ± 0.006	5.784 ± 0.008	0.6879 ± 0.0011
15	35.02 ± 0.02	5.062 ± 0.008	8.540 ± 0.009	3.687 ± 0.007	6.659 ± 0.009	0.6875 ± 0.0009
17	41.79 ± 0.02	5.559 ± 0.007	9.651 ± 0.008	4.104 ± 0.006	7.536 ± 0.008	0.6855 ± 0.0007
20	52.72 ± 0.02	6.39 ± 0.01	11.23 ± 0.01	4.824 ± 0.009	8.91 ± 0.01	0.6850 ± 0.0009
22	60.30 ± 0.06	6.94 ± 0.02	12.28 ± 0.02	5.26 ± 0.02	9.75 ± 0.02	0.6839 ± 0.0015
26	76.68 ± 0.03	8.08 ± 0.01	14.45 ± 0.02	6.19 ± 0.01	11.54 ± 0.02	0.6836 ± 0.0008
30	94.23 ± 0.06	9.13 ± 0.02	16.51 ± 0.02	7.15 ± 0.01	13.34 ± 0.02	0.6830 ± 0.0008
35	117.4 ± 0.1	10.39 ± 0.02	19.16 ± 0.02	8.18 ± 0.02	15.56 ± 0.03	0.6817 ± 0.0008
40	142.9 ± 0.2	11.70 ± 0.03	21.81 ± 0.04	9.28 ± 0.03	17.79 ± 0.05	0.6807 ± 0.0013
50	197.1 ± 0.3	14.25 ± 0.04	26.81 ± 0.05	11.50 ± 0.04	22.27 ± 0.06	0.6797 ± 0.0012
60	257.1 ± 0.4	16.70 ± 0.08	31.52 ± 0.08	13.73 ± 0.07	26.57 ± 0.09	0.6778 ± 0.0016
70	321.9 ± 0.3	19.11 ± 0.08	36.61 ± 0.07	15.88 ± 0.06	31.01 ± 0.08	0.6771 ± 0.0012
80	390 ± 1	21.3 ± 0.1	41.4 ± 0.2	17.9 ± 0.1	35.5 ± 0.2	0.6762 ± 0.0022
100	539.5 ± 0.4	26.1 ± 0.1	50.54 ± 0.09	22.2 ± 0.1	43.2 ± 0.1	0.6735 ± 0.0011

Thus, one can see that the MCRG results deviate by at most 0.07% from the exact RG findings, which is an exceptionally good agreement between the two (Monte Carlo and exact) approaches to solving the problem and thereby provides reliance on the accuracy of the MCRG results for larger  $b$ .

In figure 3 we depict our MCRG findings for the critical exponent  $y$  of the SG family of fractals as a function of  $1/b$ . In this figure, we have also graphically presented (full curve) the finite-size scaling formula for the same critical exponent

$$y_{\text{KS}} = 2 - \nu d_f \quad (16)$$

proposed in [18]. It follows from both the MCRG method and the finite-size scaling approach that  $y$  is a monotonically decreasing function of  $b$ , which means that the number of polymer contacts (crossings of the SAW paths) decreases with an increase in the homogeneous patches that comprise the SG fractals. We argue that in the region of  $b$  under study the behaviour of  $y$  is more accurately described by the MCRG findings than by the finite-size scaling formula (16). This argument springs from the fact that the MCRG results are in excellent agreement with the known exact RG results and from the fact that (16) is intrinsically a very approximate formula for finite  $b$ . Indeed, numerical analysis shows that, beginning with the fractal parameter  $b = 26$ , deviations of the values predicted by formula (16) from the MCRG findings monotonically decrease (from 5.02%, for  $b = 26$ , to 4.43%, for  $b = 100$ ). On the other hand,  $\nu \rightarrow 3/4$  and  $d_f \rightarrow 2$  when  $b \rightarrow \infty$  and, accordingly, the finite-size scaling formula (16) predicts that in this limit  $y \rightarrow 1/2$ . The available MCRG results cannot assess the limiting value  $1/2$ ; however, one should expect that an extension of the MCRG data (beyond  $b = 100$ ) can verify the simple asymptotic behaviour given by formula (16).

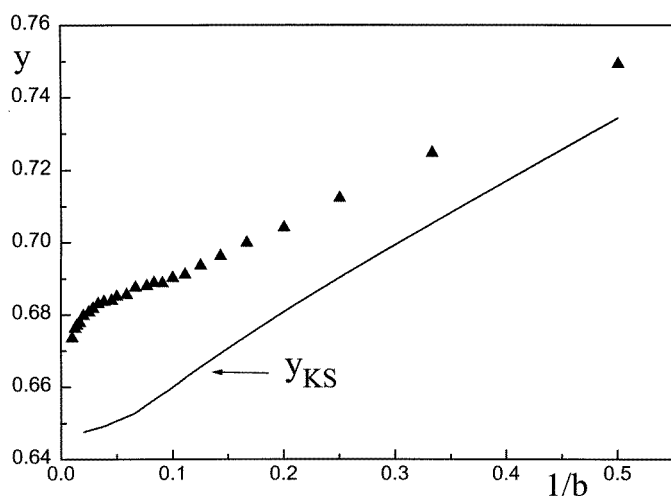


**Figure 3.** The MCRG data (full triangles) for the contact critical exponent  $y$  for the SG family of fractals. The full curve represents the finite-size scaling formula  $y_{\text{KS}} = 2 - \nu d_f$  for the same critical exponent proposed by Kumar and Singh [18]. The error bars related to the MCRG data are not depicted in the figure since in all cases studied they lie virtually within the corresponding full triangles (this is particularly relevant in the region  $2 \leq b \leq 5$ , where the largest deviation from the known exact RG values is 0.07%). On these grounds, one may argue that the full triangles represent the actual behaviour of  $y$ , whereas the full curve represents an approximate behaviour which should become correct in the limit  $b \rightarrow \infty$ .



In conclusion, we have demonstrated that the statistics of two mutually crossing SAWs on the simple family of SG fractals can be rewardingly studied by the MCRG method. In particular, the MCRG study of the contact critical exponent  $\gamma$  revealed its interesting behaviour as a function of the fractal scaling parameter  $b$ . For this reason, we argue for the necessity of similar studies on families of more complex fractals.

## References

- [1] de Gennes P G 1979 *Scaling Concept in Polymer Physics* (Ithaca, NY: Cornell University Press)
- [2] Bouchaud E and Vannimenus J 1989 *J. Physique* **50** 2931
- [3] Lapp A, Mottin M, Broseta D and Leibler L 1992 *J. Physique* II **2** 1247
- [4] Sato I, Norisuye T and Fujeta H 1987 *J. Polym. Sci. B* **25** 1
- [5] Briber R M and Bauer B J 1988 *Macromolecules* **21** 3296
- [6] de Gennes P G 1979 *J. Physique Lett.* **40** 69
- [7] Kappeler Ch, Schäfer L and Fukuda T 1991 *Macromolecules* **24** 2715
- [8] Benmouna M, Vilgis T A, Daoud M and Benhamou M 1994 *Macromolecules* **27** 1172
- [9] Witten T A and Prentis J J 1982 *J. Chem. Phys.* **77** 4247
- [10] Joanny J F, Leibler L and Ball R 1984 *J. Chem. Phys.* **81** 4640
- [11] Schäfer L and Kappeler Ch 1985 *J. Physique* **46** 1853
- [12] Benhamou M, Derouiche A and Bettachy A 1997 *J. Chem. Phys.* **106** 2513
- [13] Freed K F 1985 *J. Phys. A: Math. Gen.* **18** 871
- [14] Sariban A and Binder K 1987 *J. Chem. Phys.* **86** 5859
- [15] Dhar D 1978 *J. Math. Phys.* **19** 5
- [16] Elezović S, Knežević M and Milošević S 1987 *J. Phys. A: Math. Gen.* **20** 1215
- [17] Kumar S and Singh Y 1993 *J. Phys. A: Math. Gen.* **26** L987
- [18] Kumar S and Singh Y 1997 *J. Stat. Phys.* to be published
- [19] Kumar S, Singh Y and Dhar D 1993 *J. Phys. A: Math. Gen.* **26** 4835
- [20] Miljković V, Milošević S and Živić I 1995 *Phys. Rev. E* **52** 6314
- [21] Milošević S, Živić I and Miljković V 1997 *Phys. Rev. E* **55** 5671
- [22] Milošević S and Živić I 1991 *J. Phys. A: Math. Gen.* **24** L833
- [23] Živić I, Milošević S and Stanley H E 1994 *Phys. Rev. E* **49** 636